

Pre-test CFD simulations of the NACIE-UP BFPS test section

R. Marinari^{1*}, I. Di Piazza², N. Forgiione¹, F. Magugliani³

¹ Università di Pisa, DICI, Pisa, Italy

² ENEA FSN-ING, C.R. Brasimone, Camugnano (Bo), Italy

³ Ansaldo Nucleare, Genova, Italy

*Corresponding author. E-mail: ranieri.marinari@gmail.com

HIGHLIGHTS

- Numerical study of flow blockage phenomena in a HLM cooled pin bundle adopting ANSYS CFX code;
- The *SST-k- ω* turbulence model is adopted;
- CFD results adopted for the correct location of the instrumentation;
- Preliminary analysis for a flow blockage detection system;

KEYWORDS

Heavy liquid metals; LBE; CFD; fuel pin bundle; flow blockage

1. Abstract

The present paper is focused on the CFD pre-test analysis and design of the new experimental facility ‘Blocked’ Fuel Pin bundle Simulator (BFPS) that will be installed into the NACIE-UP (NATURAL Circulation Experiment-UPgrade) facility located at the ENEA Brasimone Research Center (Italy).

The BFPS test section will carry out suitable experiments to fully investigate different flow blockage regimes in a 19 fuel pin bundle providing experimental data in support of the development of the ALFRED (Advanced Lead-cooled Fast Reactor European Demonstrator) LFR DEMO.

The geometrical domain of the fuel pin bundle simulator was designed to reproduce the geometrical features of ALFRED, e.g. the external wrapper in the active region and the spacer grids. Pre-tests calculations were carried out by applying accurate boundary conditions; the conjugate heat transfer in the clad is also considered.

The blockages investigated are internal blockages of different extensions and in different locations: central sub-channel blockage, corner sub-channel blockage, edge sub-channel blockage, one sector blockage, and two-sector blockage.

RANS simulations were carried out adopting the ANSYS CFX commercial code with the laminar sublayer resolved by the mesh resolution. The loci of the peak temperatures and their width as predicted by the CFD simulations are used for determining the location of the pin bundle instrumentation. The CFD pre-test analysis allowed also investigating the temperature distribution in the clad to operate the test section safely.

Symbols

D	External pin diameter [mm]
f_{Darcy}	Darcy-Weisbach friction factor [-]
H	Exhagonal key of the bundle
L_{active}	Length of the heating part of the pins [mm]
L_{plenum}	Length of the mixing region downstream of a FA [mm]
L_{total}	Total length of the pin [mm]
N_{pins}	Number of pins per FA [-]

48	Nu	Nusselt number [-]
49	P/D	Pitch-to-diameter ratio [-]
50	Pr_t	turbulent Prandtl number [-]
51	Q	Maximum heating power [kW]
52	Q_{pin}	Maximum power of a pin [kW]
53	q''	Maximum het flux [MW/m ²]
54	r	radial coordinate [mm]
55	Re_{BFPS}	BFPS Reynolds number [-]
56	$T_{pin,max}$	Maximum pin temperature [°C]
57	v	Subchannel velocity [m/s]
58	y^+	dimensionless wall distance [-]
59	z	axial coordinate [mm]

60 **Acronyms**

61	AISI	American Iron and Steel Institute
62	ALFRED	Advanced Lead Fast Reactor European Demonstrator
63	BI	Blockage Index
64	BFPS	Blocked Fuel Pin bundle Simulator
65	CFD	Computational Fluid Dynamic
66	DEMO	DEMONstrator
67	ENEA	Agenzia nazionale per le nuove tecnologie, l'energia e lo sviluppo economico sostenibile
68	EU	European Union
69	FA	Fuel Assembly
70	FBR	Fast Breeder Reactor
71	FFT	Fast Fourier Transform
72	FPS	Fuel Pin Simulator
73	FP7	Framework Program 7
74	GEN-IV	Generation IV
75	HLM	Heavy Liquid Metal
76	HLMR	Heavy Liquid Metal Reactor
77	HTC	Heat Transfer Coefficient
78	HX	Heat eXchanger
79	H2020	Horizon 2020 project
80	KIT	Karlsruher Institute für Technologie
81	LBE	Lead Bismuth Eutectic
82	LEADER	Lead European Advanced Demonstrator Reactor
83	LES	Large Eddy Simulation
84	LFR	Lead Fast Reactor
85	NACIE-UP	NAtural Circulation Experiment Upgrade
86	O.D.	Outside Diameter
87	PFBR	Prototype Fast Breeder Reactor
88	RANS	Reynolds Average Navier-Stokes
89	SESAME	Thermal-hydraulics Simulations and Experiments for the Safety Assessment of MEtal cooled reactors
90	SST	Shear Stress Transport model
91	TC	ThermoCouple
92		

93 **2. Introduction**

94
95 In the context of GEN-IV heavy liquid metal-cooled reactors safety studies, the flow blockage in a fuel sub-assembly is considered
96 one of the main issues to be addressed and one of the most important and realistic accident for Lead Fast Reactors (LFR) fuel
97 assembly. The blockage in a fast reactor Fuel Assembly (FA) may have serious effects on the safety of the plant leading to the FA
98 damaging or melting. The temperature of the coolant leaving the FA is considered an important indicator of the health of the FA (i.e.

the effective heat removal) and is usually monitored via a dedicated, safety-related system (e.g. thermocouple). The external or internal blockage of the FA may impair the correct cooling of the fuel pins, be the root cause of anomalous heating of the cladding and of the wrapper and potentially impact also fuel pins not directly located above or around the blocked area. In order to model the temperature and velocity field inside a wrapped FA under unblocked and blocked conditions, detailed experimental campaign as well as 3D thermal hydraulic analyses of the FA is required. The root causes of the FA blockage are aggregation of solid matter (oxides), dislodged from its intended location or generated in the coolant, transported inside and along with the coolant's flow; this matter could stop inside the FA (mainly because of its narrow spaces) and interfere with the coolant flowing inside the FA. The main consequence of the blockage is a reduction of the coolant flow rate through the FA. Blockage can be instantaneous (when a large enough piece of material obstructs a portion of the channels of the FA) or time dependent (when the aggregation of solid matter piles up in the channels of the FA). For grid-spaced FAs, an internal blockage is generally located in the first grid and it has a flat-like shape (Schultheiss, 1987). FAs are usually designed with a number of inlet slots to prevent a complete and instantaneous blockage.

Fuel Assembly blockage, total or partial, has been extensively analyzed since the early days of fast reactors. While many of these studies refer to Sodium Fast Reactors, the results may be a starting point for LFRs too. The focus of these analyses is to determine the effects of a blockage on the temperature (cladding and coolant) and pressure (coolant) inside the FA as well as at the outlet of the subassembly, and to find the optimal detection techniques. Investigations carried out within the LEADER FP7 EU project showed that the maximum clad temperature to avoid long-term creep in the Ti15-15 cladding material is 650 °C (Weisenburger, 2013).

Wey et al. (1982) described the development of a Monte Carlo model capable of generating real time temperature signals from a specified input temperature profile and turbulent velocity field. The model used multi-particle batches, which permit calculations simulating heat dissipation processes. Various Sodium Loop experiments are outlined which were used to validate the model in turbulent pipe and jet flows. For the latter, a multistage technique was used which enabled modeling of axial variation of the turbulence field. The technique has also been used to predict temperature signals at the outlet of subassemblies with blockages of various sizes at center and corner positions. A simple assessment of the viability of detecting such blockages with a single centrally located sensor is presented.

Hae-Yong Jeong et al. (2014) analyzed the temperature rise across each subassembly in order to detect the formation of a significant size of blockage. The blockage detection logic of the Prototype Fast Breeder Reactor (PFBR) generates an alarm signal when the assembly-wide temperature rise deviates 5 K from the pre-determined value and scram signal for a deviation greater than 10 K. The paper proposed a concept of Blockage Index (BI) by adopting a kernel function of Gaussian type to take advantage of the thermal-hydraulic information in neighboring subassemblies. With the blockage index, a distance-weighted temperature changes for each subassembly is defined. Combining the blockage index for each subassembly into a core wide map of blockage indices, useful information are gathered to determine whether any blockage is introduced or not at some location of subassembly. It is also possible to adjust the range of influence by performing sensitivity studies on reference distance in advance to select a distance factor which describes the blockage phenomena most correctly for the given subassembly design.

Seung-Hwan Seong et al. (2006) used the LES turbulence model in the ANSYS CFX code for analyzing the temperature fluctuation in the upper plenum. After analyzing the temperature fluctuations in the upper plenum, a basic design requirement was established for the flow blockage detection system through a FFT analysis and a statistical analysis. They concluded that response time of a measuring device was less than 13 ms and that it should cover a high temperature range of 1000 K. In addition, the resolution of the thermocouple should be less than 2 K and its location should be within 25 cm from the exit of each assembly.

Nomoto et al (1980) installed thermocouple temperature sensors above the central region of the core in the JOYO experimental sodium fast reactor to monitor the outlet coolant temperature of 115 subassemblies. Subassembly outlet coolant temperature distributions were obtained under various power levels, different main cooling system flowrates, and unequal reactor inlet temperatures from the two cooling loops. In addition, coolant temperature and flowrate distributions at the subassembly outlet measured in a zero power experiment are presented.

Maity et al. (2011) carried out thermal hydraulic studies to understand temperature dilution (defined as the difference between thermocouple reading and real temperature at the same location) experienced by core-temperature monitoring system of a sodium cooled fast reactor. The three-dimensional computational model was validated against experimental results of a water model. The analysis indicates the maximum possible dilution in fuel and blanket subassemblies to be 2.63 K and 46.84 K, respectively. Shifting of thermocouple positions radially outward by 20 mm with respect to subassembly centers leads to an overall improvement in accuracy of thermocouple readings. It is also seen that subassembly blockage that leads to 7% flow reduction in fuel subassembly and 12% flow reduction in blanket subassembly can be detected effectively by the core-temperature monitoring system.

Di Piazza et al. (2014) carried out a CFD study on fluid flow and heat transfer in the Lead-cooled Fuel Pin Bundle of the ALFRED LFR DEMO. The authors developed a detailed thermo-fluid dynamic analysis at various levels of geometrical blockage. In particular, the closed hexagonal grid-spaced fuel assembly of the LFR ALFRED was modeled and computed. While the spacer grids were not included in the model, a conservative analysis has been carried out based on the current main geometrical and physical features. Results indicate that critical conditions, with clad temperatures $\approx 900^\circ\text{C}$, are reached with geometrical blockage larger than 30% in terms of area fraction. The results show that two main effects can be recognized: a local effect in the wake/recirculation region downstream the blockage and a global effect due to the lower mass flow rate in the blocked subchannels. The former effect gives rise

to a temperature peak behind the blockage and it is dominant for large blockages (>20%), while the latter effect determines a temperature peak at the end of the active region and it is dominant for small blockages (<10%). The blockage area was placed at the beginning of the active region, in such a way that both abovementioned phenomena can be seen. Different mass flow rates and different levels of geometrical blockage were imposed from preliminary system code simulations. Transient analyses with fully resolved SST-omega turbulence model were carried out and results indicate that a blockage of ~15% (in terms of blocked area) leads to a maximum clad temperature around 800°C, and this condition is reached in a characteristic time of 3–4 s without overshoot. Local clad temperatures around 1000°C can be reached for blockages of 30% or more. CFD simulations indicate that blockages (in terms of blocked area) greater than 15% could be detected by placing thermocouples in properly selected locations in the plenum region of the FA.

Kirsch (1975) presented experimental and theoretical investigations of the flow and temperature distribution in local recirculating flows in rod bundles, downstream of a blockage. A mean coolant temperature in this recirculation zone can be calculated from the dimension of the recirculation zone and the mass exchange rate with the main flow. Similarity analysis for recirculating flow in a simple geometry without rods shows that with a sufficiently high Reynolds number, similar geometry and similar heat distribution, the dimensionless temperature fields (in the bulk region) in recirculating flows are equal and independent of the Reynolds and Prandtl numbers. This result is also observed to be true for rod bundles, justifying temperature distribution measurements to be performed with water instead of sodium. Otherwise, the experimental study of temperature field on pins' surfaces due to a blockage, requires a liquid metal as coolant.

This work is focused on a CFD pre-test analysis of the new experimental test section called 'Blocked' Fuel Pin bundle Simulator (BFPS) that will be installed into the NACIE-UP (NATURAL Circulation Experiment-UPgrade) facility located at the ENEA Brasimone Research Center (Italy). RANS simulations were carried out adopting the ANSYS CFX commercial code. The loci of the peak temperatures and their width as predicted by the CFD simulations are used for determining the correct location of the pin bundle instrumentation.

3. The NACIE-UP facility

The results of the flow blockage simulations presented in this paper will be used to select the location of the thermocouples and other probes in the experiments carried out by a proper BFPS test section installed in the NACIE-UP facility.

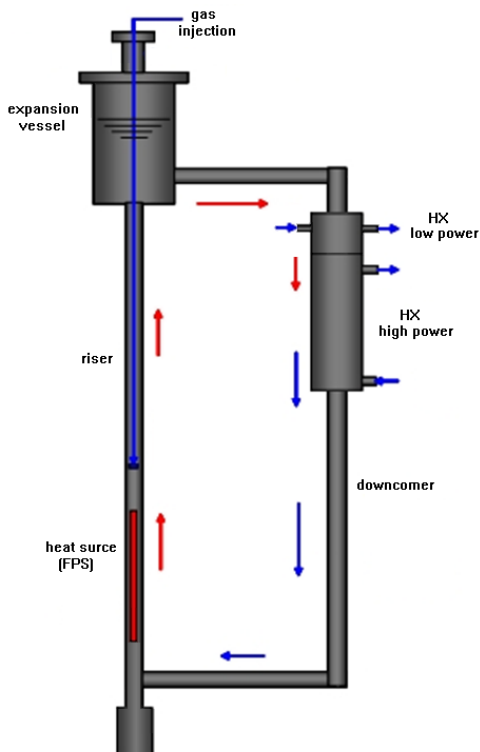
NACIE-UP is a rectangular loop, which allows to perform experimental campaigns in the field of the thermal-hydraulics, fluid-dynamics, chemistry control, corrosion protection and heat transfer and to obtain correlations essential for the design of nuclear power plant cooled by heavy liquid metals. It basically consists of two vertical pipes of O.D. 2.5 in. (63.5 mm)), working as riser and down comer, connected by two horizontal pipes of O.D. 2.5 in. (63.5 mm)). The whole height of the facility is about 7.7 m, while the horizontal length is about 2.4 m. A section of the facility is devoted to place the prototypical fuel pin bundle simulator (FPS) test sections in the lower part of the riser. In the last experimental campaign, performed in 2015, a wire-wrapped 19-pin 250 kW FPS was mounted. The test section for the blockage experiment will be placed in place of the previous one. A proper heat exchanger is placed in the upper part of the down comer.

NACIE-UP is made of stainless steel (AISI 304) and can use both lead and the eutectic alloy LBE as working fluid (about 2000 kg, 200 l of total capacity). It was designed to work up to 550°C and 10 bar. The difference in height between the center of the heating section and the center of the heat exchanger is about 5.5 m and it is very important for the natural circulation. In the riser, an argon gas injection device ensures a driving force to sustain forced convection in the loop.

A schematic layout of the primary circuit is reported in Figure 1. The facility includes:

- The Primary side filled with LBE, with 2.5 in. (63.5 mm) pipes. It consists of two vertical pipes, working as riser and down comer, two horizontal pipes and an expansion tank;
- A Fuel Pin Simulator (19-pins) 250 kW maximum power, placed in the bottom of the riser of the primary side (it will be replaced by the new BFPS test section);
- A shell and tube HX with two sections, operating at low power (5-50 kW) and high power (50-250 kW). It is placed in the higher part of the down comer;
- A prototypical thermal flow meter (0-20 kg/s), located in the cold leg;
- 3 bubble tubes to measure the pressure drops across the main components and the pipes;
- Differential pressure transducers (1 mbar accuracy) for the test section;
- Several bulk thermocouples to monitor the temperature along the flow path in the loop;
- The secondary side, filled with water at 16 bar, connected to the HX, shell side. It includes a pump, a pre-heater, an air-cooler, by-pass and isolation valves, and a pressurizer with cover gas;
- An ancillary gas system, to ensure a proper cover gas in the expansion tank, and to provide gas-lift enhanced circulation;
- A LBE draining section, with 0.5 in. (12.7 mm) pipes, isolation valves and a storage tank.

208 The ancillary gas system has the function to ensure the cover gas in the expansion tank and to manage the gas-lift system in the riser
 209 for enhanced circulation regime.
 210



211 **Figure 1 Technical drawing and main dimension of the NACIE-UP loop.**
 212
 213

214 **4. The BFPS test section**

215 The Blocked Fuel Pin Simulator (BFPS) test section was designed in order to study the local and bulk effects of an internal blockage
 216 in a 19-pin LFR ALFRED DEMO-like FPS.
 217

218 The heat source will consist of 19 electrical pins with an active length $L_{active} = 600$ mm ($L_{total} = 2000$ mm, including the *non-active*
 219 length) and a diameter $D = 10$ mm. The pitch to diameter ratio is $P/D = 1.4$. The maximum external pin heat flux will be ≈ 0.7 MW/m².
 220 The pins will be placed on a hexagonal layout by a suitable wrapper, while two grids will maintain the pin bundle in the correct
 221 position. The total power of the pin fuel bundle is ≈ 250 kW.

222 This fuel pin bundle configuration is relevant for the ALFRED's core thermal-hydraulic design. ALFRED is a flexible fast spectrum
 223 research reactor (300 MW_{th}). The main parameters of BFPS test section and ALFRED core are reported in Table 1 for comparison.

Parameter	BFPS	ALFRED FA
D [mm]	10	10.5
P/D	1.4	1.32
Q [kW]	250	-
Q_{pin} [kW]	13	-
q'' [MW/m ²]	0.7	0.7-1
v [m/s]	0.8	1.1

N_{pins}	19	127
$L_{active} [mm]$	600	600
$L_{plenum} [mm]$	500	500

Table 1 Comparison of the main parameters between the BFPS test section and ALFRED core

The goals of the experimental campaigns planned on the NACIE-UP loop facility with the BFPS bundle are:

- measurement of the pin wall temperature both with and without blockage by embedded thermocouples;
- measurement of the subchannel temperature;
- Heat Transfer Coefficient (HTC) evaluation;
- axial temperature profiles in the wrapper and in the subchannels;
- check the presence of hot spots and localized peak of temperature;
- evaluation of the thermal mixing above the pin bundle;

A preliminary drawing of the BFPS test section is shown in Figure 2. A spacer grid is located at the beginning of the active region where the coupling flange is present. Without blockage, the test section allows to characterize the flow and the heat transfer in the FA. By opening the coupling flange located upstream the active region and by closing grid subchannels by caps, proper blockages at the beginning of the active region can be achieved.

The central spacer grid will be the key component of the flow blockage experimental campaign and it is specifically described in the following.

The central grid in its unblocked configuration is reported (viewed from the top) in Figure 3, with inlet pipe and pin numeration for reference. The grid has an external circular shape and two notches for the correct position of the component between the central flanges. The inner hexagonal key of the grid has the same dimension of the bundle one ($H= 62$ mm). The 19 circular holes have the same dimension and pitch of the bundle while the septa among them and the grid will have the lowest thickness achievable without compromise the structural integrity of the component and the right installation of the caps; anyway, the septa location is fixed.

For the flow blockage configuration, several caps will be displaced on the different holes of the central grid; those caps will be small thin plates of appropriate shape positioned by moving rods from the bottom to fix a configuration.

Pins and LBE temperature downstream the blockage will increase due to the lower cooling rate in this region. The extension and magnitude of those hot regions are strictly related to the blockage type and blocked flow area of the grid.

The test section will be instrumented with 100 thermocouples. The location of the thermocouples in the system is fixed according to the results of the present pre-test analysis.

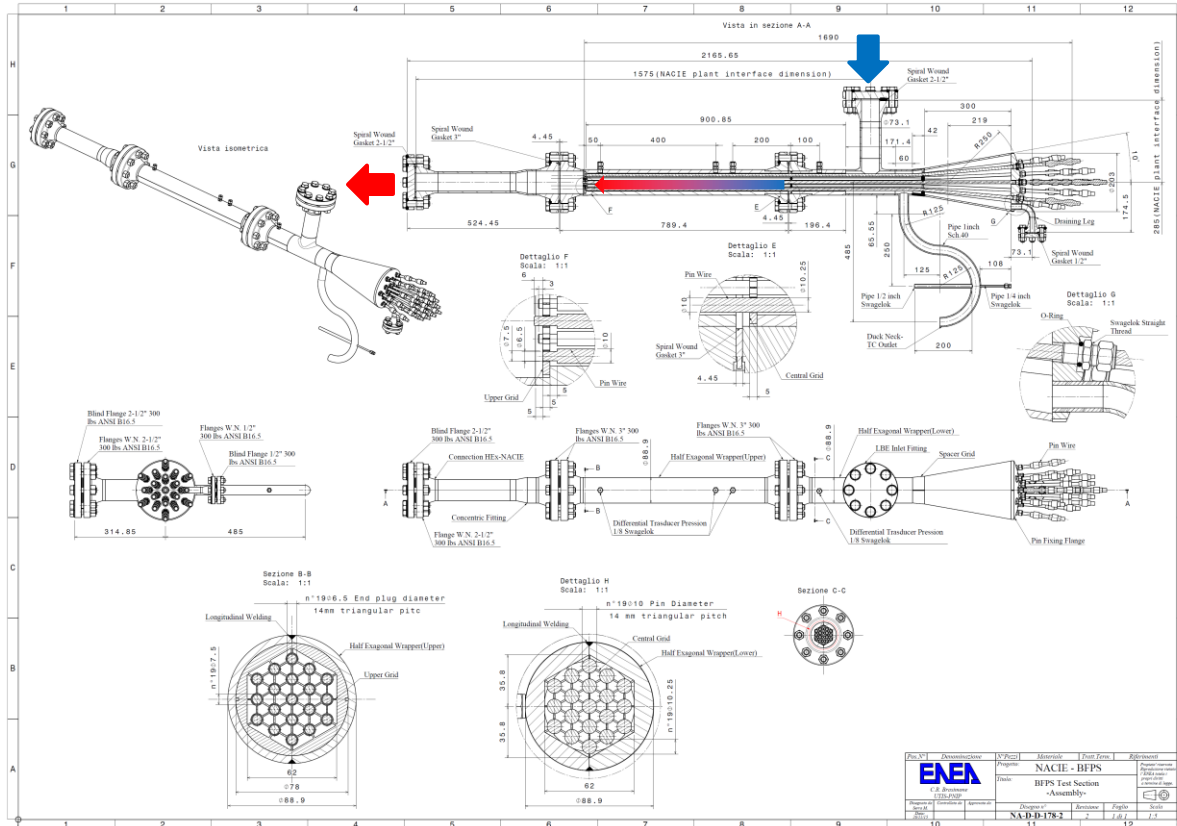


Figure 2 Preliminary mechanical drawing of the BFPS test section.

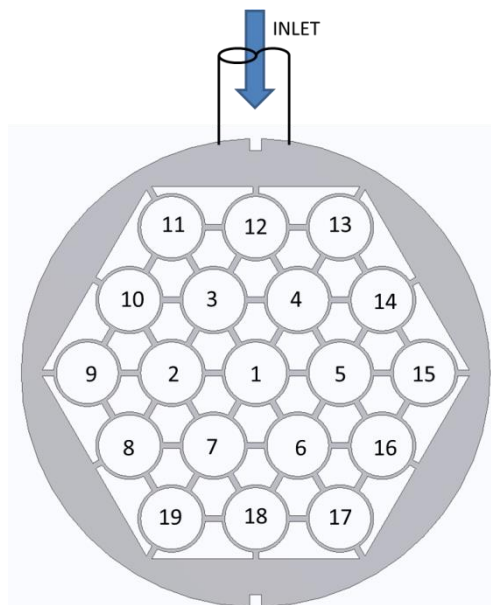


Figure 3 Sketch of the central grid in unblocked configuration (viewed from the top)

5. Numerical models and methods

For the CFD pre-test analysis of the experiment, the BFPS test section was modeled. A sketch of the computational domain is shown in Figure 4 which includes (from bottom to top) the developing region, the active region (“Pins”), and the mixing region downstream of the FA. The inlet bend is not included in these simulations because its position is not fixed yet. Anyway, further sensitivity analyzes including the inlet bend, have shown that the previous simulations (without bend) were conservative (predicting higher temperature behind the blockage) but anyway hot-points locations and critical regions for instrumentation are the same. The conjugate heat transfer in the hexagonal wrapper and in the coupling flange was also accounted. The importance of the conjugate heat transfer in this kind of test sections was assessed in previous works; see Di Piazza (2015) and Doolaard (2015). The meshes developed are fully unstructured both in the fluid and solid domains. The number of nodes is inflated near the solid walls for the resolution of the viscous sub-layer ($y^+=1$ for the highest Re case) and at least 4 nodes in the viscous sub-layer.

The general-purpose code ANSYS CFX 15 was used for all the numerical simulations presented in this paper. The code employs a coupled technique, which simultaneously solves all the transport equations in the whole domain through a false time-step algorithm. The linearized system of equations is preconditioned in order to reduce all the eigenvalues to the same order of magnitude.

Constant mass flow rate, temperature at inlet and pressure at outlet were applied as boundary conditions for the simulations. The external surface of the hexagonal wrapper is considered adiabatic, being insulated with 100 mm of thermal insulator.

The SST (Shear Stress Transport) $k-\omega$ model by Menter (1994) was extensively used in this paper. It is formulated to solve the viscous sub-layer explicitly, and requires several computational grid points inside the viscous sub-layer. The turbulent Prandtl number was set to 1.5, according to the literature suggestions (Cheng and Tak, 2006). Buoyancy forces were neglected (conservative approach).

Four meshes have been developed and tested to perform a mesh independence analysis, with 10, 15, 19, 24 million nodes on the whole domain and $y^+=1$ for all the computational grids (see Table 2). Because the results for fluid flow, heat transfer and temperature (maximum and at outlet) of the unblocked case were comparable to a very high degree among the 4 meshes, the mesh C with 19 million nodes was selected representing a good compromise between computational requirements and numerical accuracy. Two views of mesh C are shown in Figure 5.

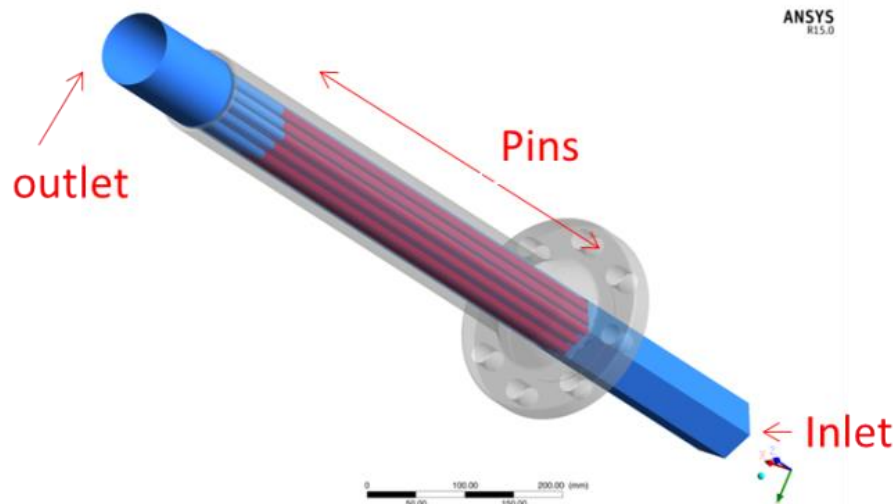


Figure 4 Sketch of the computational domain.

Mesh	Million nodes [-]	f Darcy [-]	Nu [-]	$T_{pin,max}$ [°C]
A	10	0.01182	23.86	267.6
B	15	0.01144	17.31	269.8
C	19	0.01130	16.48	272.4
D	24	0.01131	16.52	272.6

Table 2 Mesh adopted for the grid-independence study, with the main overall output parameters.

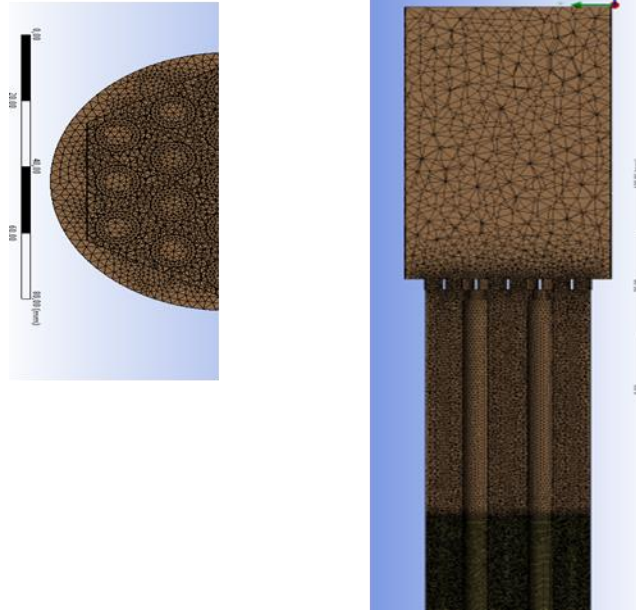


Figure 5 Computational mesh C adopted for the simulations

Four different blockage types were chosen for the pre-test analysis. These are shown in Figure 6 where type 0 refers to the unblocked case. The mechanical method for implementing the blockage (i.e. how to block the flow in the subchannels) is via a stainless steel cap fixed to the grid spacer with push&pull rods, properly fitted according to the type and location of the blockage. A pre-test matrix was prepared for defining the different blockage types at different mass flow rates. In the test cases presented here, the mass flow rate was kept constant at 16 kg/s, corresponding to 108 kg/s in the ALFRED FA (75% of the nominal flow rate), and it is the maximum flow rate achievable in the NACIE-UP facility (maximum axial extension of the wake region behind the blockage). The power of the FPS was 94.2 kW to have an inlet-outlet temperature increase of 40°C (for BFPS safe operation). The inlet temperature is 200°C, to protect test section from damages during the experiments.

Only the most relevant cases of the complete computational test matrix are presented here, and are summarized in Table 3.

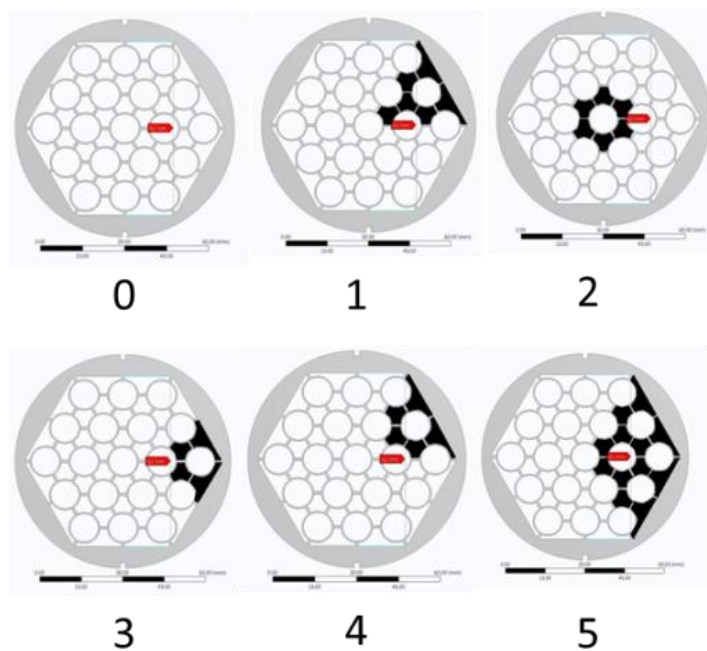
Case	Blockage type	Mass flow rate [kg/s]	Re _{BFPS} [-]	Power [kW]	Inlet temperature [°C]
0	0	16	46663	94.2	200
1	1	16	46663	94.2	200
2	2	16	46663	94.2	200
3	3	16	46663	94.2	200
4	4	16	46663	94.2	200
5	5	16	46663	94.2	200

Table 3 Test matrix presented in the paper.

The mass flow rate was kept constant at the different degree of blockage. This is justified by the fact that in the real ALFRED FA geometry, blockage degrees up to 30% would not affect significantly the flow rate (Di Piazza, 2014) and the interest is focused on the local phenomena.

Figure 7 shows the clad temperature distribution in the active region for the unblocked case 0. The temperature gradient is basically axial as expected with a maximum temperature of the cladding is 261°C, with hot points in the corner regions. Figure 8 (left) shows the clad temperature distribution in the region behind the blockage for blockage type 1 (sector blockage, case 1), while Figure 8 (right) shows the LBE temperature in the stagnation region immediately after the blockage. A local temperature peak (Figure 8 right) in the region 100 mm behind the blockage is clearly visible with a maximum temperature of about 360°C, well above the maximum temperature of the unblocked case. The local temperature increase due to the blockage is about 150°C. As evidenced in other computational and theoretical studies (Di Piazza, 2015) (Kirsch, 1975) (Roelofs, 2012), the reason for the local temperature peak is the vortex generated downstream by the obstacle represented by the blockage; in the central, stagnation point of the vortex heat is

315 exchanged only by conduction and the temperature increases. This hydrodynamic effect is shown in Figure 9, where temperature field
 316 and secondary flow field (left) are shown at the cross-sections at $z=10, 20, 30, 45$ mm from the blockage (located at $z=0$ mm at the
 317 beginning of the active region, first grid) for case 1 (sector blockage). A vortex due to the blockage obstacle is clearly evidenced
 318 between $z=10$ mm and 45 mm with a maximum of the secondary flow (see Figure 9 (center) at $z=45$ mm). The temperature field
 319 shows a peak value in planes $z= 20, 30$ mm in the stagnation region.
 320 Figure 10 shows the temperature distribution for all the cases simulated at 16 kg/s at the outlet section in the mixing region; please
 321 note that the color scales adopted are different. The trace of the blockage is clearly visible in all cases. Figure 12 shows the
 322 temperature distribution in a radial line at the outlet section. For the unblocked case (Case 0), mixing guarantees a maximum spatial
 323 difference of temperature of about 1.5°C, while in the blocked cases the spatial temperature distribution clearly shows the location of
 324 the underlying blockage with a temperature difference of 15 °C for Case 1 and 28 °C for Case 5. The relevant difference both in the
 325 value of the temperature in a specific location as well as in the spatial distribution of the temperature confirms the possibility to detect
 326 the internal blockage at this level of blockage by putting thermocouples in properly selected locations of the mixing region of the
 327 BFPS test section (Naveen Raj, 2016).
 328 The experimental investigation of the temperature gradients in the mixing region of the test section is crucial to confirm this
 329 possibility.
 330
 331



332
 333

Figure 6 Different blockage types: (0) unblocked; (1) sector; (2) central; (3) corner; (4) edge; (5) two sectors.

334
335

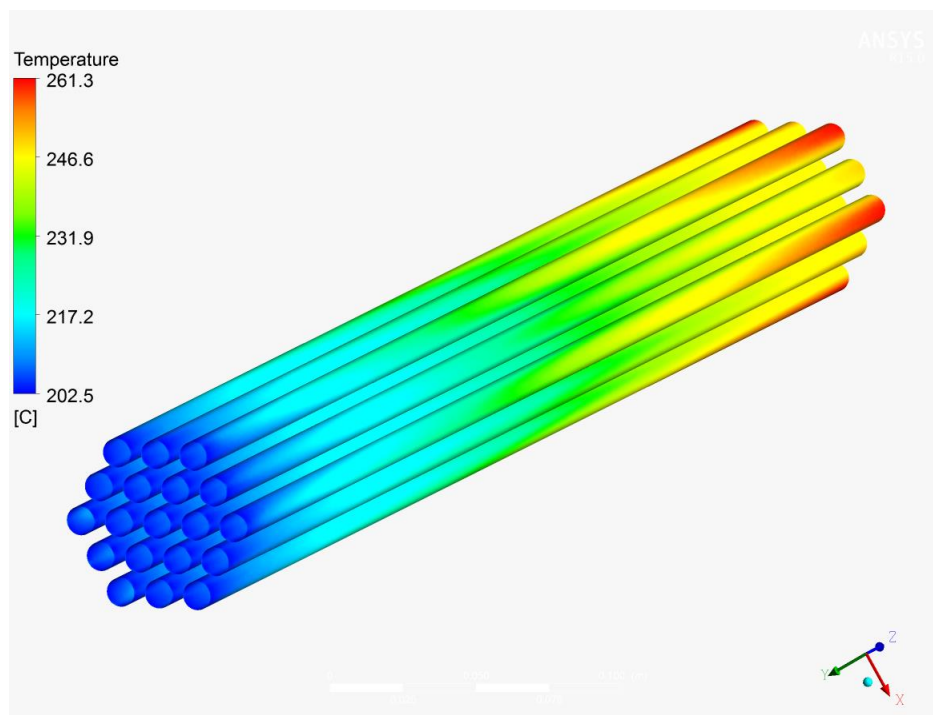
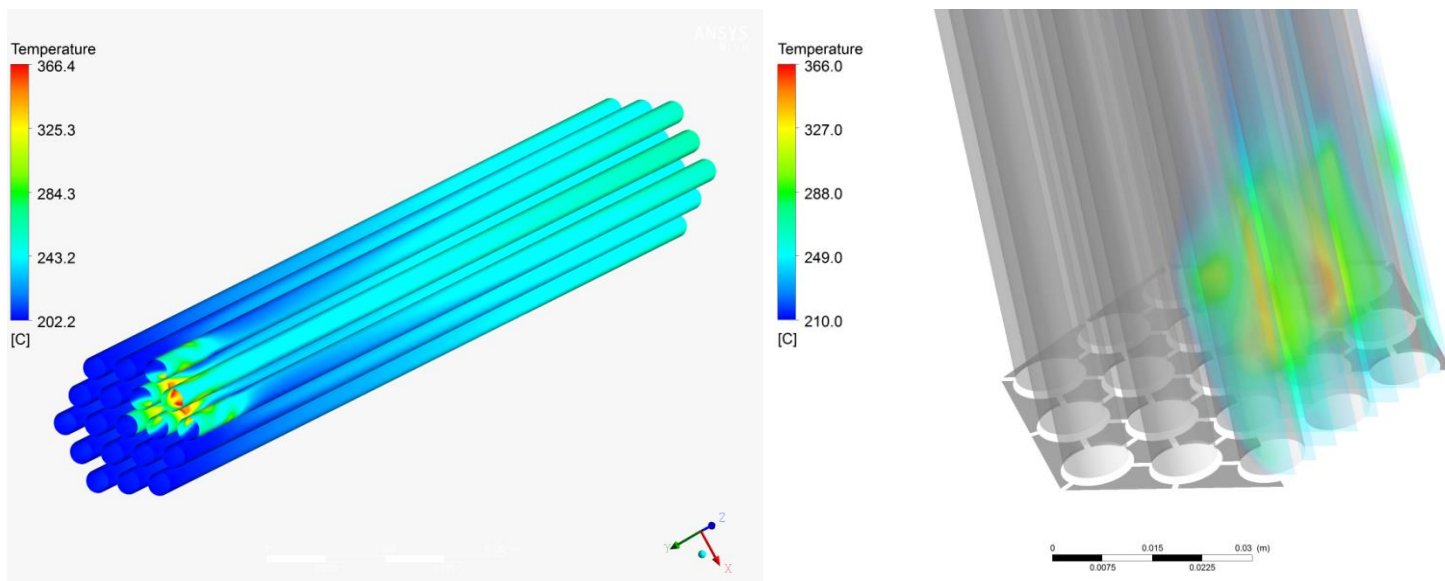


Figure 7 Pin clad temperature field in the unblocked case.

336
337
338



339
340
341

Figure 8 Clad temperature field in the region behind the blockage (Case 1) on the left and LBE temperature in the stagnation region on the right.

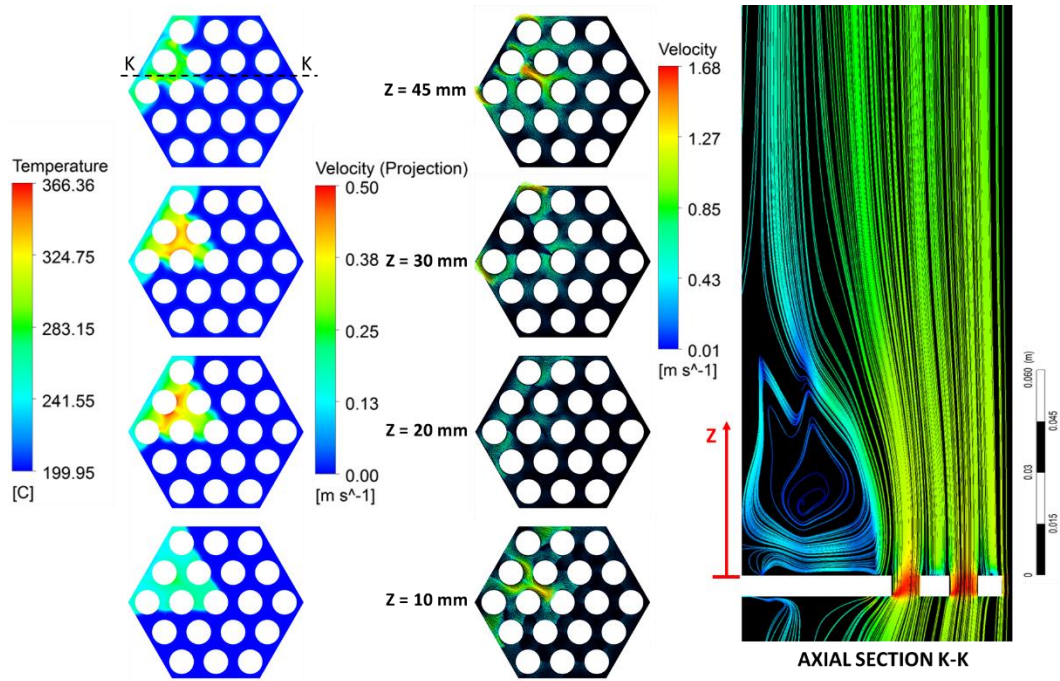


Figure 9 Temperature field and secondary vector plot (left) on four different planes located at $z=10, 20, 30, 40, 45$ mm from the beginning of the active region. Recirculation region over the sector blockage (right).

342
343
344
345

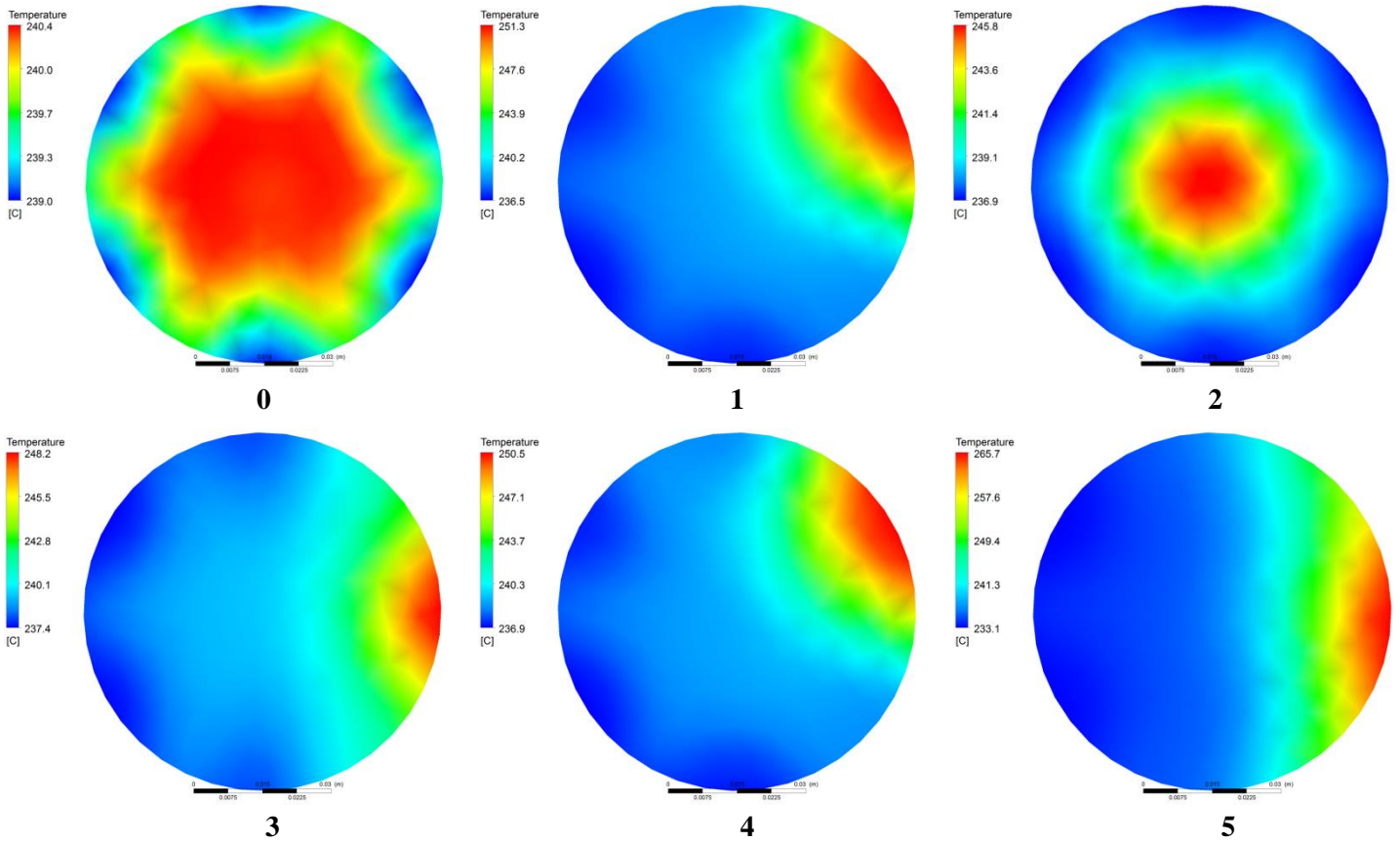


Figure 10 Temperature distribution on the outlet section of the mixing region (16 kg/s) for case 0 (unblocked), 1 (sector blockage), 2 (central blockage), 3 (corner blockage), 4 (edge blockage), 5 (two sector blockage).

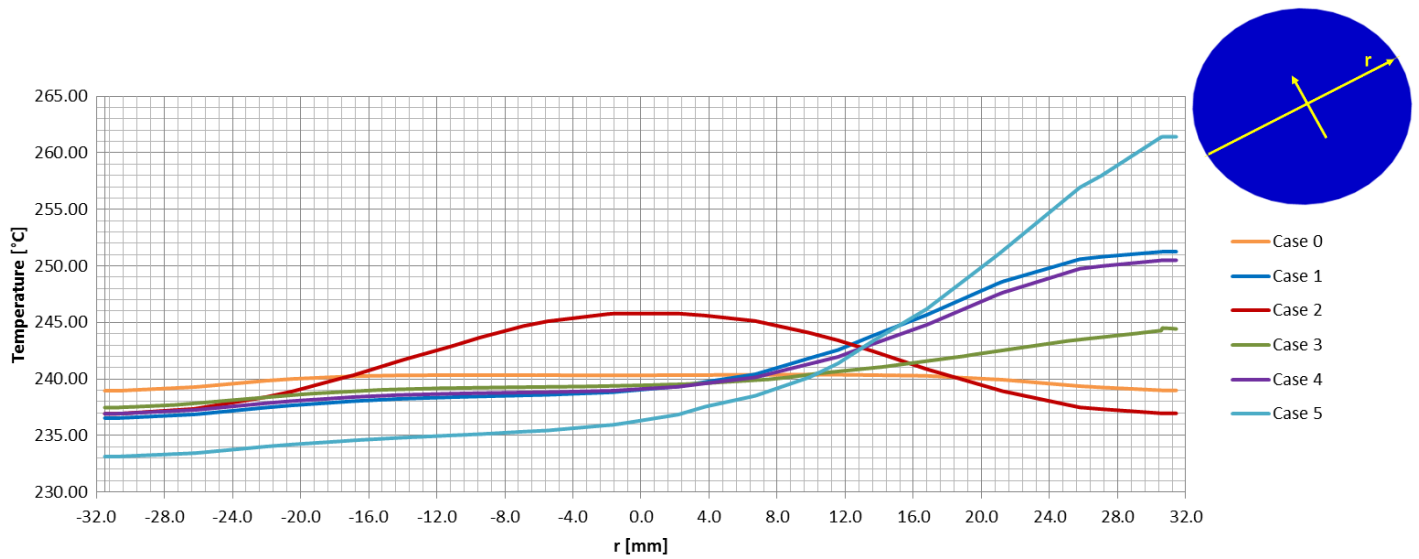
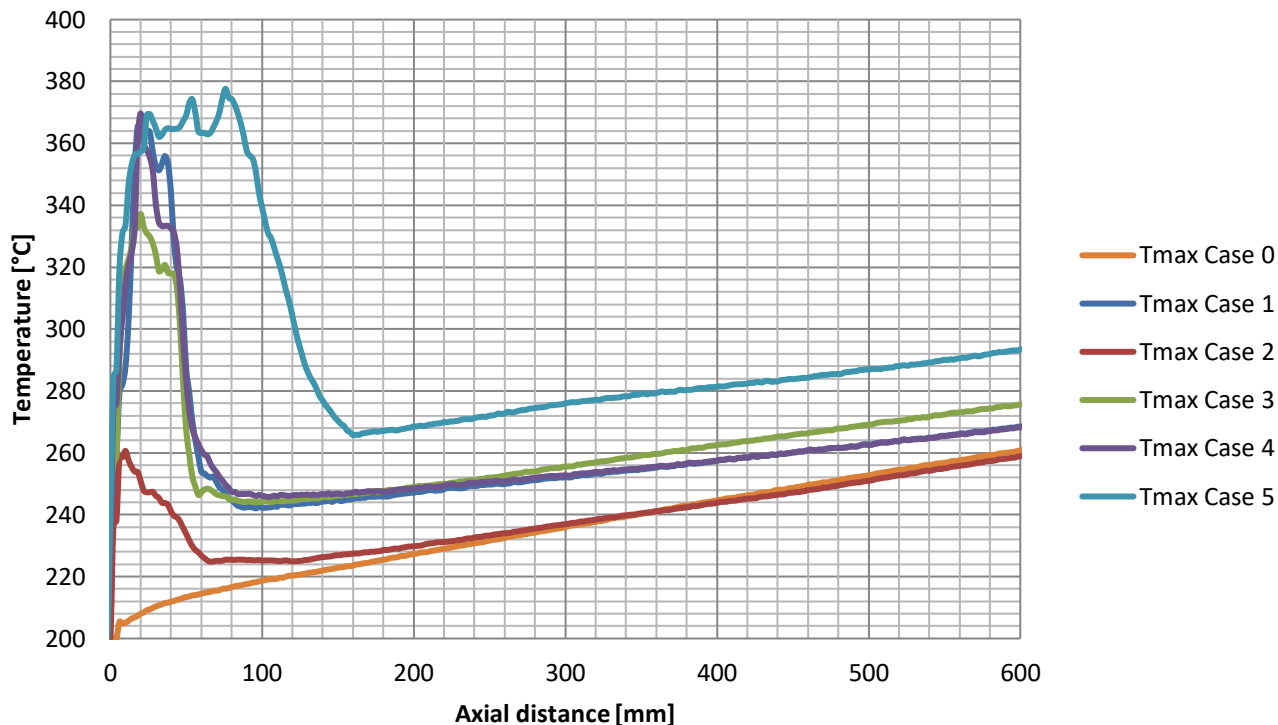


Figure 11 Temperature profile for all the cases simulated on a line placed at the outlet section of the model (top right sketch)

Figure 12 shows the maximum temperature profiles along the stream wise axial direction for all simulated cases, with the axial distance starting from the beginning of the active region. Most of the cases have a similar maximum temperature behind the blockage

358 around 360°C, about 150°C difference with respect to the unblocked case. The region of influence behind the blockage is limited to
 359 50-100 mm in most cases, and 200 mm for the larger two-sector blockage (case 5). This result is in line with previous studies (Di
 360 Piazza, 2015) (Kirsch, 1975) and the region of influence is tied to the extension of the blocked area. Typically, an elongated
 361 recirculation vortex of aspect ratio 2-3 behind the blockage is present. A larger blockage will lead to a longer vortex and to a larger
 362 region of influence.
 363



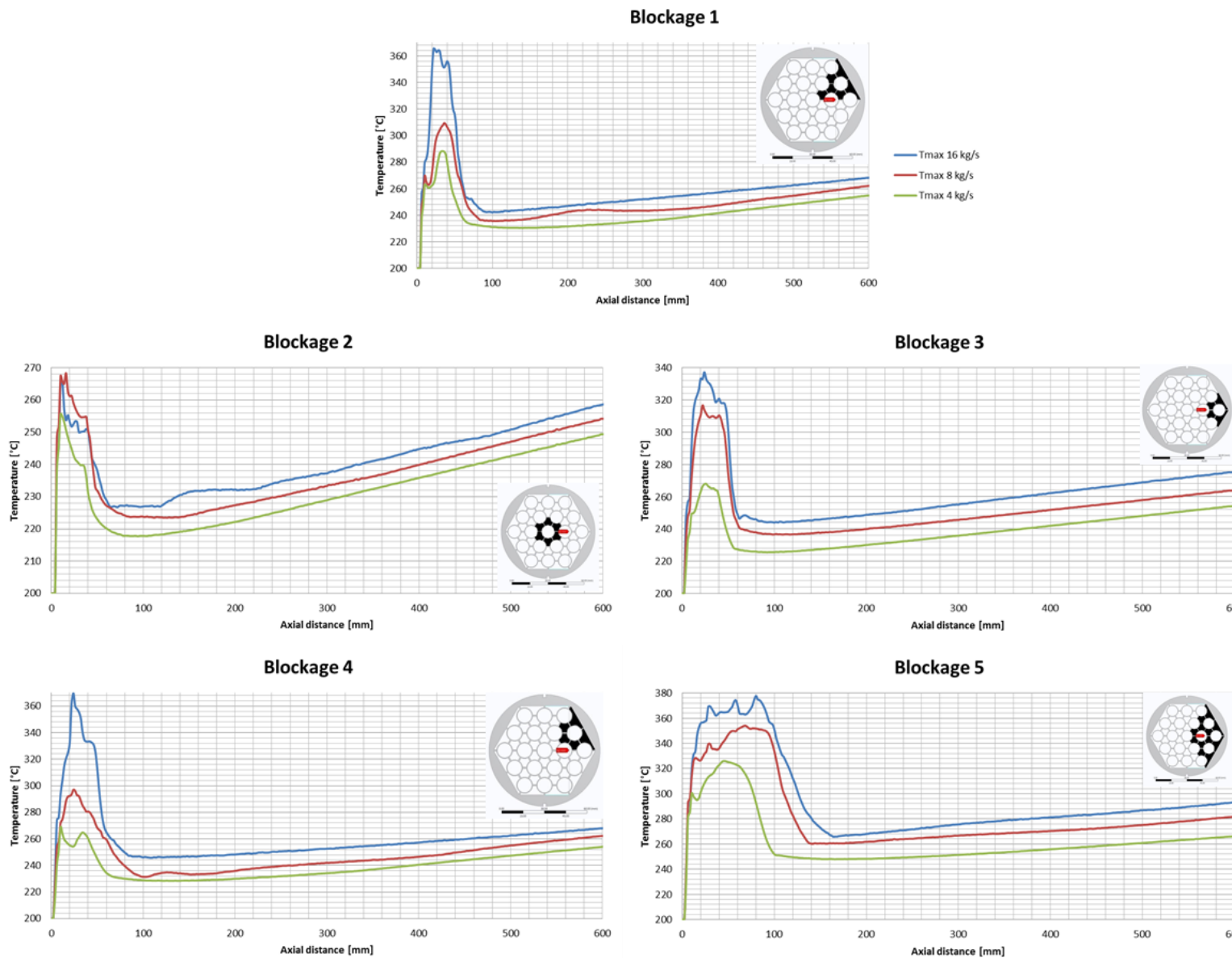
364 **Figure 12 Maximum temperature profile along the stream-wise axial direction for the 6 cases investigated.**

365
 366
 367 The previous numerical simulations with different blockage types were also performed at lower mass flow rates (4 kg/s and 8 kg/s)
 368 keeping the same inlet-outlet bulk temperature increase (40 °C); their main input data are reported in Table 4.
 369

Case	Blockage type	Mass flow rate [kg/s]	Re _{BFPS} [-]	Power [kW]	Inlet temperature [°C]
0-8	0	8	23332	47.1	200
1-8	1	8	23332	47.1	200
2-8	2	8	23332	47.1	200
3-8	3	8	23332	47.1	200
4-8	4	8	23332	47.1	200
5-8	5	8	23332	47.1	200
0-4	0	4	11666	23.57	200
1-4	1	4	11666	23.57	200
2-4	2	4	11666	23.57	200
3-4	3	4	11666	23.57	200
4-4	4	4	11666	23.57	200
5-4	5	4	11666	23.57	200

370 **Table 4 Test matrix of the pre-test study**
 371

372 The most interesting parameter to be compared among the different cases is the maximum temperature on the pins and the extent of
 373 the “hot region” keeping a constant blockage type. This is shown in the different graphs of Figure 13. The axial dimension of the
 374 recirculation region is not strongly dependent from mass flow rate but it is mainly tied to the blockage area and type; in particular its
 375 maximum width is achieved for blockage 5 (two sector blockage) and 16 kg/s where it reaches 200 mm at least.
 376 On the other hand, the peak cladding temperature increases with the blocked area and with the mass flow rate. This latter effect on the
 377 mass flow rate is due to the fact that the test matrix is designed with a constant inlet-outlet bulk temperature, and therefore the heat
 378 flux increases linearly with the mass flow rate. For example, for blockage 1, the power of the FPS is 23.57, 47.1, 94.2 kW for 4, 8, 16
 379 kg/s, respectively.
 380 The separate influence of mass flow rate on the temperature peak for a fixed blockage configuration is shown in Figure 14 in the case
 381 of blockage 1 (sector) and a constant power of 47.1 kW. The temperature peak increases when the mass flow rate decreases, while the
 382 extension of the hot region is nearly the same, as clearly expected from intuition.
 383



384
 385 **Figure 13 Comparison of maximum temperature and ‘hot region’ extension for different blockages and at different mass flow**
 386 **rates.**
 387
 388

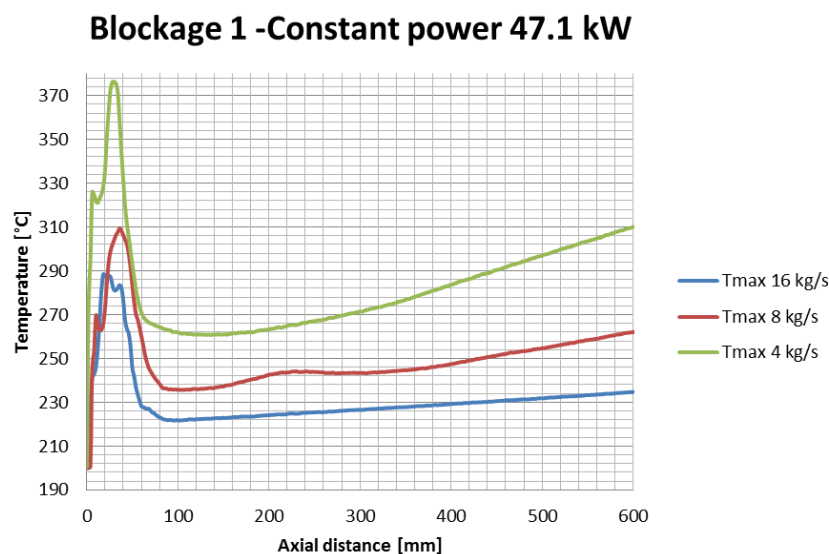


Figure 14 Maximum temperature along the axis at different mass flow rates and at a constant bundle power of 47.1 kW.

The present results suggest how to position of the instrumentation in the test section. The blocked region will be monitored with 0.35 mm wall-embedded thermocouples, most of them located on the hottest pins in the region of influence. The remaining thermocouples are positioned in order to measure bulk and wall temperatures in the different subchannels and to characterize heat transfer in different conditions. The generic section of the FPS was divided in 36 subchannels, see Figure 15, corresponding to the grid passages at the beginning of the active region, see Figure 3 for comparison. The bundle was divided in 6 sectors from A to F. The code identifying the subchannel, e.g. B2, refers to the sector (e.g. letter 'B') and to the rank (e.g. number '2').

The thermocouple locations are shown in Figure 16, with the instrumented pins colored in red. Pins 1, 2, 5, 15 will be equipped with wall embedded thermocouples on a generatrix parallel to the pin axis, and sub-channel B2 will be instrumented with 0.5 mm bulk thermocouples.

Sixteen different levels will be considered for the four generatrices and the sub-channel: $z = 10, 20, 30, 40, 50, 60, 70, 80, 90, 100, 150, 200, 300, 400, 500, 600$ mm starting from the beginning of the active region of the pins. Plane at $z = 550$ mm will be instrumented as in the following to characterize the heat transfer in the unblocked case:

- pins 1, 2, 4, 5, 7, 9, 14, 15 will be instrumented with wall embedded thermocouples;
- sub-channels B1, B2, B5, E1, E5 and the corner sub-channels across B5/C4 and E5/F4 will be instrumented with bulk thermocouples 0.5 mm thickness placed at the center of the subchannel;
- An additional bulk thermocouple of 0.35 mm thickness is placed in subchannel B1 at a distance of 1 mm from the wall.

This instrumentation will allow to collect data on temperature distribution in the case of blockage and to characterize the heat transfer in the unblocked condition by measuring cold spots in the side subchannels and the heat transfer coefficients. This will be a fundamental characterization of the ALFRED FA for the different ranks of subchannels.

Additional instrumentation (24 TCs) will be placed in the 500 mm mixing region of the test section to collect data for CFD code validation and HLM thermal mixing. TCs will be placed downstream the FPS at different axial, radial and azimuthal positions.

This choice is justified by the temperature trend at the outlet section of the CFD model for the different blockage types and different mass flow rates simulated and reported in Figure 11, Figure 17 and Figure 18 for the 16, 8 and 4 kg/s cases respectively. The radial temperature distribution in the mixing region over the pin bundle, in particular its shape and temperature maxima, could be adopted as a track for detecting the faulted FAs (affected by blocked sub-channels).

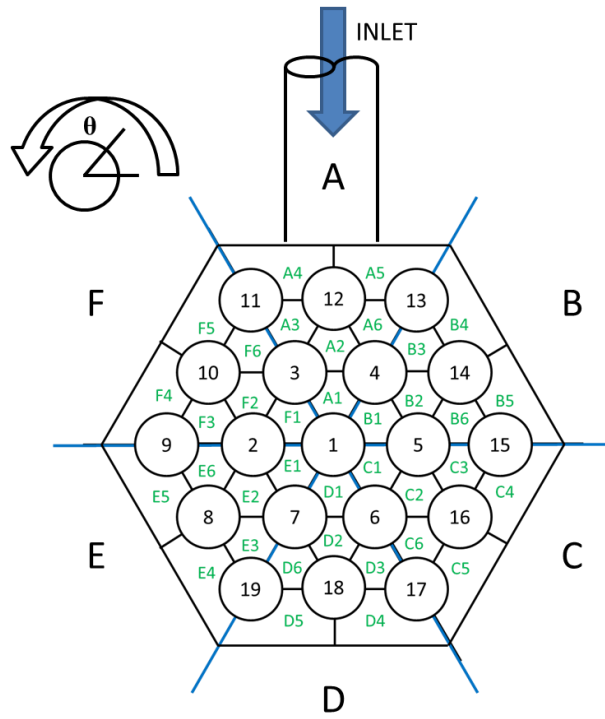


Figure 15 Sketch of a section of the new FPS for the NACIE-UP facility viewed from the top.

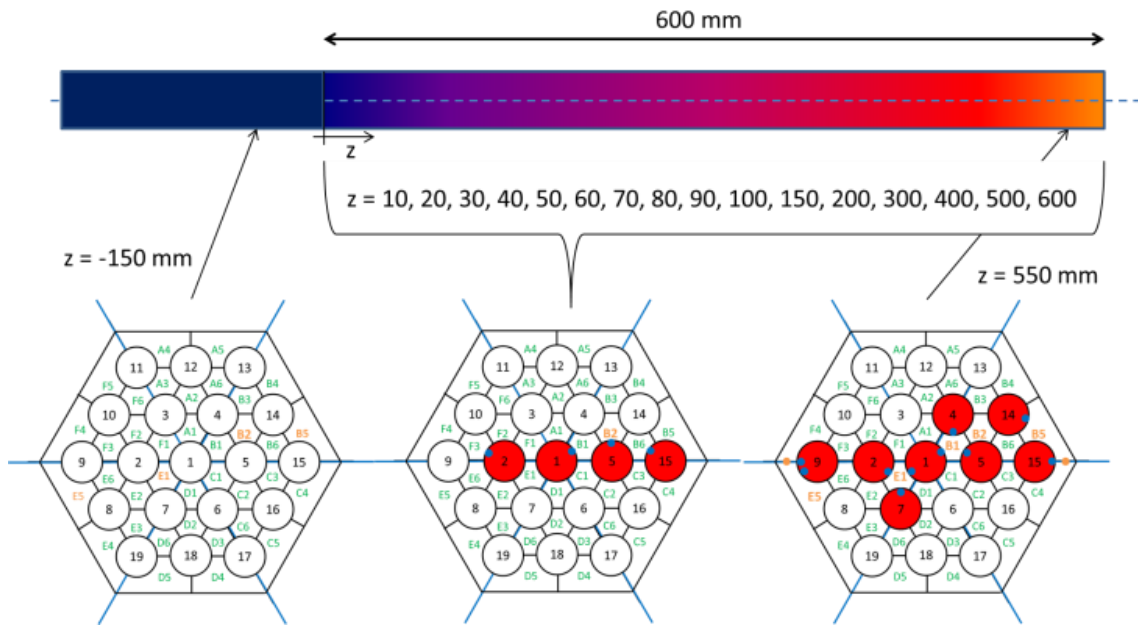
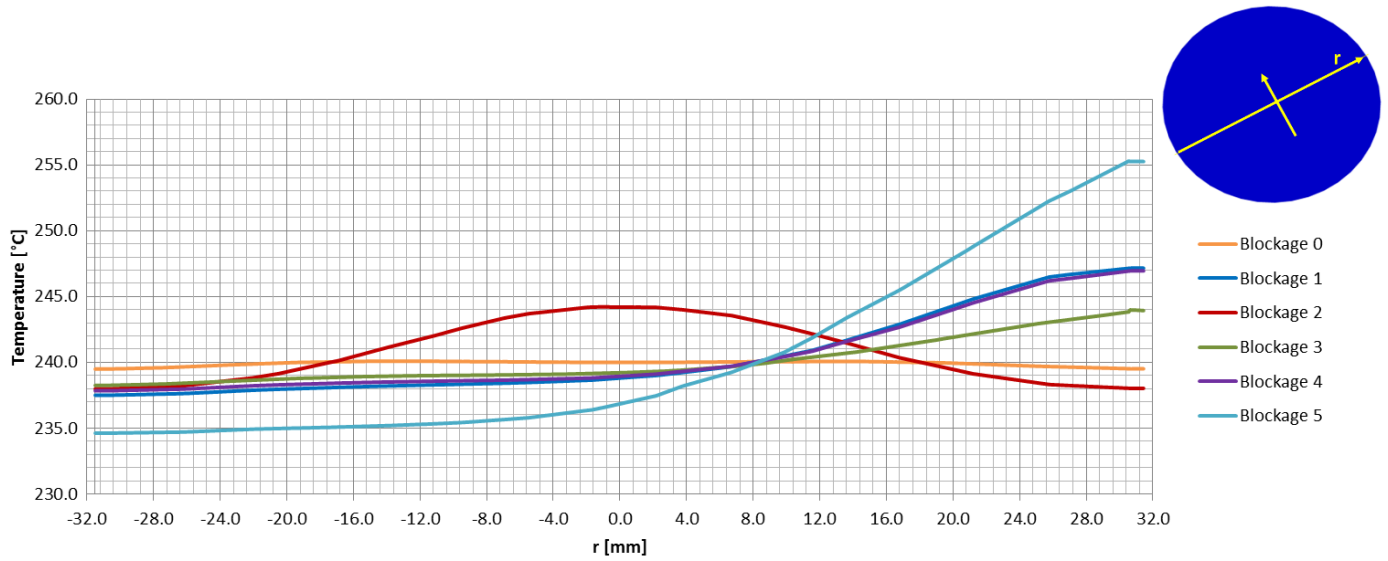


Figure 16 Overall pin bundle TC instrumentation

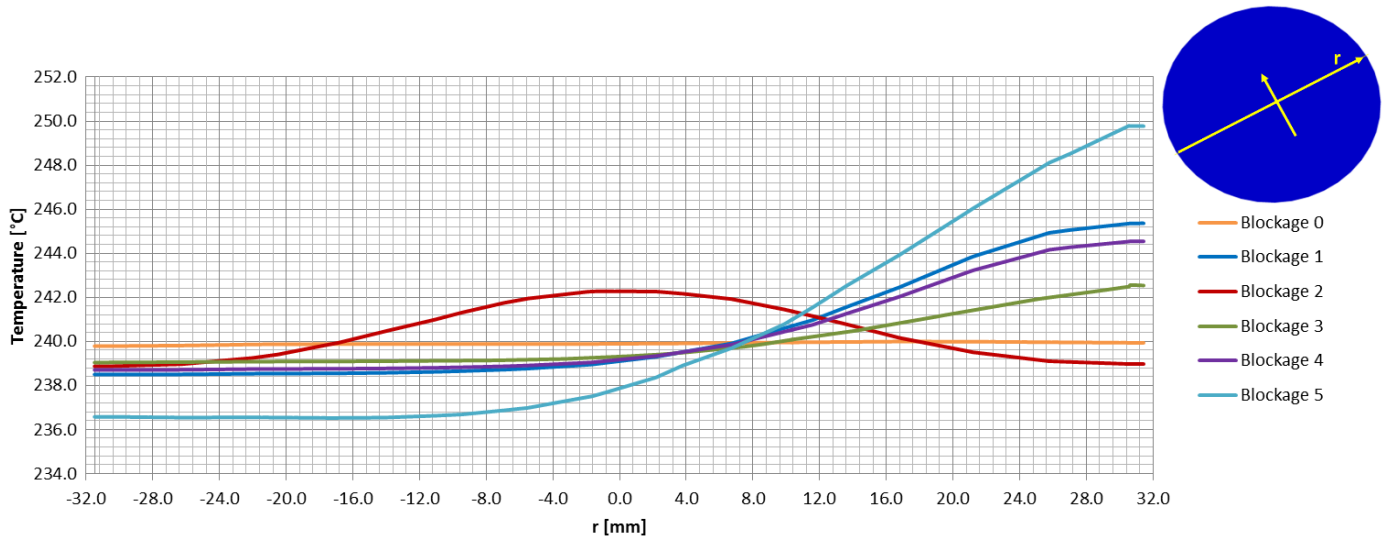
422
423
424
425

426
427
428
429
430



431
432
433
434
435

Figure 17 Temperature profile on a line placed at the outlet section of the model (top right sketch) for all the blockage types at 8 kg/s.



436
437
438
439
440

Figure 18 Temperature profile on a line placed at the outlet section of the model (top right sketch) for all the blockage types at 4 kg/s.

6. Conclusions

441
442
443
444
445
446
447
448
449

The present paper is focused on the CFD pre-test analysis of the ‘Blocked’ Fuel Pin bundle Simulator (BFPS) that will be installed into the NACIE-UP facility located at the ENEA Brasimone Research Center (Italy). The BFPS test section will be installed into the existing NACIE-UP loop facility aiming to carry out suitable experiments to fully investigate the effects of different flow blockage regimes in a 19 fuel pin bundle providing experimental data in support of the ALFRED LFR DEMO development. In particular, the fuel pin bundle simulator (BFPS) cooled by lead bismuth eutectic (LBE), was conceived with a thermal power of about 250 kW, a uniform wall heat flux up to 0.7 MW/m². It consists of 19 electrical pins placed on a hexagonal lattice with a pitch to diameter ratio of 1.4 and a diameter of 10 mm.

450 Several blockage types (central, sector, side, corner) were simulated in the grid at the beginning of the active region with a subchannel
451 velocity around 0.8 m/s, relevant for LFR. The aim of this pre-test calculation is to evidence basic phenomena and correctly place the
452 instrumentation to capture relevant gradients.

453 Pre-test CFD analysis shows the same basic phenomena of previous studies on larger bundles (Di Piazza, 2014) and documented in
454 literature (Schultheiss, 1987) (Kirsch, 1975). A strong local effect is evident behind the blockage area leading to an elongated vortex
455 with a decrease of heat transfer between the coolant and the cladding. Consequently, in the region of influence behind the blockage, a
456 temperature rise occurs both for the coolant and for the cladding. The extension of the region of influence is about 200 mm in the
457 present case, but it scales with the extension of the blockage.

458 The local overheating is strictly dependent on the operational conditions. For the present case, safe conditions were chosen for the
459 experimental FPS, i.e. 92 kW power with 40°C inlet-outlet temperature rise with an inlet temperature of 200°C.

460 The local temperature increase due to the blockage is about 150°C for most of the cases in the present conditions.

461 The pre-test analysis confirms that blockage could be detected via properly placing the instrumentation, (wall-embedded and bulk
462 thermocouples located along the active region, most of them in the region of influence of the blockage). Blockage could be detected
463 placing TCs in the mixing region of the BFPS test section.

464 With this instrumentation, the BFPS experiment will provide unique local data on the FA blockage for HLM cooled configurations, by
465 providing a database for code validation to extend the CFD blockage analysis to a full FA, and giving indications on the detection
466 methods.
467

468 7. Acknowledgments

469 This work was performed in the framework of the H2020 SESAME project. This project has received funding from the Euratom
470 research and training program 2014-2018 under grant agreement No 654935.
471

472 8. References

473 Cheng, X., Tak, N.I., 2006. CFD analysis of thermal-hydraulic behavior of heavy liquid metals in sub-channels. Nucl.
474 Eng. Des. 236, 1874-1885.

475 Di Piazza, I., Magugliani F., Tarantino, M., Alemberti A., 2014. A CFD analysis of flow blockage phenomena in
476 ALFRED LFR demo fuel assembly. Nucl. Eng. Des. 276, 202–215.

477 Di Piazza, I., Marinari, R., “CFD PRE-TEST ANALYSIS OF THE FUEL PIN BUNDLE SIMULATOR
478 EXPERIMENT IN THE NACIE-UP HLM FACILITY” 16th International Topical Meeting on Nuclear Reactor
479 Thermal - Hydraulics, NURETH-16, August 30-September 4, 2015, Hyatt Regency Chicago.

480 Doolaard, H.J., Shams, A., Roelofs, F., Van Tichelen, ,K., Keijers, S., De Ridder, J., Degroote, J., Vierendeels, J., Di
481 Piazza, I., Marinari, R., Merzari, E., Obabko, A., Fischer, P., “CFD BENCHMARK FOR A HEAVY LIQUID METAL
482 FUEL ASSEMBLY” 16th International Topical Meeting on Nuclear Reactor Thermal - Hydraulics, NURETH-16,
483 August 30-September 4, 2015, Hyatt Regency, Chicago.

484 Greef, C.P., 1979. Temperature fluctuations: An assessment of their use in the detection of fast reactor coolant
485 blockages. Nucl. Eng. Des. 52, 35-55.

486 Hae-Yong Jeon, Moon-Ghu Park, Seung-Hwan Seon, Jae-Ho Jeong, Effectiveness of Blockage Index for the
487 Detection of Blockage in an SFR Subassembly, Transactions of the Korean Nuclear Society Spring Meeting, Jeju,
488 Korea, May 29-30, 2014.
489
490
491
492
493
494
495
496

497 Kirsch, D., 1975. Investigations on the flow and temperature distribution downstream of local coolant blockages in
498 rod bundle subassemblies. Nucl. Eng. Des. 31, 266-279.
499

500 Maity, R.K., Velusamy, K., Selvaraj, P., Chellapandi, P., 2011. Computational fluid dynamic investigations of partial
501 blockage detection by core-temperature monitoring system of a sodium cooled fast reactor. Nucl. Eng. Des. 241,
502 4994-5008.
503

504 Marinari, R., Ghionzoli, P.B., Forgiione, N., Di Piazza, I., Tarantino, M., Magugliani, F., Alemberti, A., Borreani, W.,
505 CFD pre-test analysis and design of the NACIE-UP BFPS fuel pin bundle simulator, Proceedings of the 24th
506 International Conference on Nuclear Engineering ICONE24 June 26-30, 2016, Charlotte, North Carolina, USA.
507

508 Menter, F. R., 1994. Two-Equation Eddy-Viscosity Turbulence Models for Engineering Applications. AIAA Journal
509 32(8), 1598-1605.
510

511 Naveen Raj, M., Velusamy, K., Maity, R. K., 2016. Thermal hydraulic investigations on porous blockage in a
512 prototype sodium cooled fast reactor fuel pin bundle, Nucl. Eng. Des. 303, 88–108.
513

514 Nomoto, S., Yamamoto, H., Sekiguchi, Y., Tamura, S., 1980. Measurement of subassembly outlet coolant temperature
515 in the JOYO experimental fast reactor. Nucl. Eng. Des. 62, 233–239.
516

517 Roelofs, F., Gopala, V.R., Chandra, L., Viellieber, M., Class, A., 2012. Simulating fuel assemblies with low resolution
518 CFD approaches, Nucl. Eng. Des. 250, 548-559.
519

520 Schultheiss, G.F., 1987. On local blockage formation in sodium cooled reactors. Nucl. Eng. Des. 100, 427-433.
521

522 Seung-Hwan Seong, 2006. Establishment of the design requirements for a flow blockage detection system through a
523 LES analysis of the temperature fluctuation in the upper plenum. Annals of Nuclear Energy 33, 62-70.
524

525 Weisemberger, A., Muller, G., Alemberti, A., Summary of HLM reactor materials ,LEADER FP7 WP6 report, 2013.
526

527 Wey, B.O.; Hughes, G.; Overton, R.S, Prediction of temperature fluctuations at the outlet of a blocked subassembly,
528 Proceedings of the L.M.F.B.R. safety topical meeting, 1982.
529
530
531